Princeton Plasma Physics Laboratory

PPPL- 4428

PPPL- 4428

Recent Fast Wave Coupling and Heating Studies on NSTX, with Possible Implications for ITER

J.C. Hosea, R.E. Bell, E. Feibush, R.W. Harvey, E.F. Jaeger, B.P LeBlanc, R. Maingi, C.K. Phillips, L. Roquemore, P.M. Ryan, G. Taylor, K. Tritz, E.J. Valeo, J. Wilgen, J.R. Wilson, and the NSTX Team

July, 2009

PPPL PRINCETON PLASMA PHYSICS LABORATORY

Prepared for the U.S. Department of Energy under Contract DE-AC02-09CH11466.

Princeton Plasma Physics Laboratory
Report Disclaimers

Full Legal Disclaimer

Trademark Disclaimer

PPPL Report Availability

Princeton Plasma Physics Laboratory:

http://www.pppl.gov/techreports.cfm

Office of Scientific and Technical Information (OSTI):

http://www.osti.gov/bridge

Related Links:

U.S. Department of Energy

Office of Scientific and Technical Information

Fusion Links

Recent Fast Wave Coupling and Heating Studies on NSTX, with Possible Implications for ITER

J.C. Hosea[a], R.E. Bell[a], E. Feibush[a], R.W. Harvey[b], E.F. Jaeger[c], B.P LeBlanc[a], R. Maingi[c], C.K. Phillips[a], L. Roquemore[a], P.M. Ryan[c], G. Taylor[a], K. Tritz[d], E.J. Valeo[a], J. Wilgen[c], J.R. Wilson[a], and the NSTX Team

[a]*Princeton Plasma Physics Laboratory, Princeton University, Princeton, NJ 08543, USA*
[b]*CompX, Del Mar, CA 92014, USA*
[c]*Oak Ridge National Laboratory, Oak Ridge, TN 37831, USA*
[d]*Johns Hopkins University, Baltimore, MD 21218, USA*

Abstract. The goal of the high harmonic fast wave (HHFW) research on NSTX is to maximize the coupling of RF power to the core of the plasma by minimizing the coupling of RF power to edge loss processes. HHFW core plasma heating efficiency in helium and deuterium L-mode discharges is found to improve markedly on NSTX when the density 2 cm in front of the antenna is reduced below that for the onset of perpendicular wave propagation ($n_{onset} \propto B*k_{||}^2/\omega$). In NSTX, the observed RF power losses in the plasma edge are driven in the vicinity of the antenna as opposed to resulting from multi-pass edge damping. PDI surface losses through ion-electron collisions are estimated to be significant. Recent spectroscopic measurements suggest that additional PDI losses could be caused by the loss of energetic edge ions on direct loss orbits and perhaps result in the observed clamping of the edge rotation. Initial deuterium H-mode heating studies reveal that core heating is degraded at lower k_ϕ (- 8 m^{-1} relative to 13 m^{-1}) as for the L-mode case at elevated edge density. Fast visible camera images clearly indicate that a major edge loss process is occurring from the plasma scrape off layer (SOL) in the vicinity of the antenna and along the magnetic field lines to the lower outer divertor plate. Large type I ELMs, which are observed at both k_ϕ values, appear after antenna arcs caused by precursor blobs, low level ELMs, or dust. For large ELMs without arcs, the source reflection coefficients rise on a 0.1 ms time scale, which indicates that the time derivative of the reflection coefficient can be used to discriminate between arcs and ELMs.

Keywords: RF Heating, Electron Energy and Confinement Time, Spherical Torus
PACS: 52.50.Qt, 52.55.Fa

I. INTRODUCTION

Efficient RF heating and current drive are needed in ST devices and ultimately in ITER. This requires good coupling of the RF power to the core plasma with minimal deposition in the edge region to avoid erosion on the antenna, wall and limiters [e.g., 1 – 3], as well as in the divertor scrape off regions [4,5]. Under high-harmonic fast wave (HHFW) heating conditions, the GENRAY [6] and AORSA [7] RF wave models show that even at the lowest toroidal wavenumbers of interest, $k_\phi \sim 3$ m^{-1}, the waves entering the core plasma are damped in about half an orbit around the machine,

and wave fields are very low near the center stack [8,9]. Since single-pass damping is very large, edge power loss must occur prior to the fast waves entering the last closed flux surface (LCFS). Consequently, NSTX serves as an ideal platform for separating HHFW RF power deposition in the core and the edge [8,9].

The HHFW system on NSTX is designed to facilitate good toroidal spectral selectivity [8,9]. It consists of a 12 element array antenna covering ~ 90° of the outer toroidal region of the vessel, with six decoupled 30 MHz power sources, that generate well defined directed wave spectra when the phases, ϕ_A, between adjacent antenna elements are ± 150°, ± 90° and ± 30° (k_ϕ = ± 13 m^{-1}, ± 8 m^{-1} and ± 3 m^{-1}, respectively). The power coupling efficiency to the core L-mode plasma is found to fall off at lower k_ϕ when the edge density ~ 2 cm in front of the antenna exceeds the onset density for wave propagation perpendicular to the magnetic field ($n_{onset} \propto B * k_{||}^2/\omega$). This indicates that the edge loss processes are enhanced by the higher RF fields near n_{onset}, where the perpendicular wave group velocity is zero. Core heating has been enhanced by reducing the edge density with a variety of conditioning techniques, including lithium injection [10], so that efficient heating can now be maintained to k_ϕ values as low as ~ 5 m^{-1} (ϕ_A = -60°) in deuterium (Fig.1) [9]. Significant HHFW heating of deuterium plasma for the low wavenumber k_ϕ = -3 m^{-1} has been obtained for the first time on NSTX, as indicated by the diamond point at ϕ_A = -30° in Fig. 1, albeit at reduced heating efficiency since the edge density is still above the onset value. Pushing n_{onset} far from the antenna has permitted high $T_e(0)$ values up to ~ 5 keV to be produced in both helium and deuterium plasmas in support of the study of high-k turbulence properties [11]. Finally, better control of the edge density has permitted heating of the core electrons in H-mode deuterium plasmas for the first time. These recent heating results are presented in some detail in Ref. 12 at this conference.

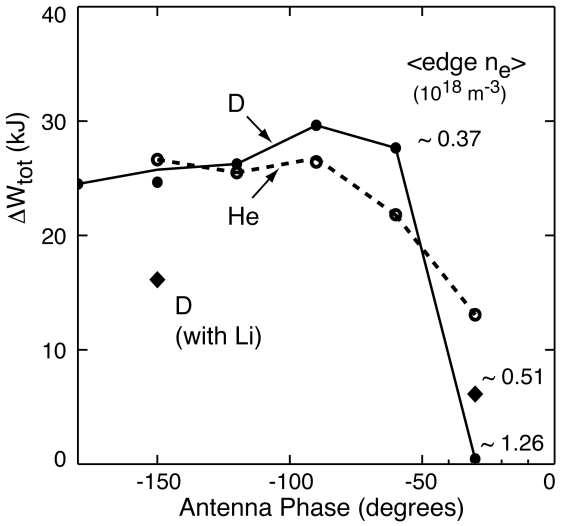

FIGURE 1. RF-induced increments in electron stored energy comparable in both He-4 (P_{RF} ~ 1.8 MW, 80 ms pulse) and D (P_{RF} ~ 1.1 MW, 230 ms pulse) discharges. Diamonds indicate results obtained with shorter RF pulses (P_{RF} ~ 1.3 MW, 67 ms pulse) in D discharges with Li injection. Time averaged Thomson scattering edge density, <edge n_e> at R = 156.2 cm, is shown for the -60° and -30° deuterium points. (B_ϕ = 0.55 T, I_p = 600 kA in He-4, I_p = 650 kA in D)

In this paper, the focus is on further investigations of the possible RF power loss processes in the edge plasma. Many edge loss processes are probably involved, including propagating and reactive wave driven losses, associated collision and RF sheath losses, and parametric decay instability (PDI) heating via ion Bernstein wave excitation. Previous edge rotation diagnostic (ERD) measurements for helium discharges have provided qualitative estimates that approximately 16% to 23% of the RF power, increasing somewhat with wavelength, could be lost via PDI heated ions

that are coupling their energy to poorly confined edge electrons through ion-electron collisions [13, 14]. However, the direct loss of these PDI produced energetic ions in the plasma edge could provide an additional loss channel, and although the loss due to this effect has not been quantified, evidence that it is present is described in Section II.

The coupling of significant power to the edge plasma via propagating fast wave fields is indicated by the clear increase in the edge loss in H-mode plasmas for longer wavelength, similar to the L-mode case, as presented in Section III. Visible camera views of a major loss channel from the scrape off layer (SOL) in front of the antenna to the outer divertor plate are also presented and discussed in the context of propagating field generated losses. Reactive fast wave fields are necessarily contributing to the edge losses, as well, due to the large (up to ~ 39°) magnetic field pitch in the edge plasma of NSTX. However, it might be expected that these fields generally peak very close to the antenna and should be less dependent on the location of the onset density relative to the front face of the antenna.

The response of HHFW power coupling to the presence of ELMs will be presented in Section III. It would appear that RF arcs in the antenna can lead to large ELMs and that in the absence of these arcs, the RF power can be applied during large ELMs by employing a reliable arc/ELM discrimination technique. Implications of the current research results for ITER ICRF heating are briefly discussed in Section IV.

II. PARAMETRIC DECAY INSTABILITY INDUCED RF LOSSES

Excitation of ion Bernstein waves via the PDI has been found to lead to substantial edge ion heating, as measured by the ERD diagnostic [13]. Edge ions including He II, C III, C VI and Li II are heated and have a "hot" component in poloidal temperature that can reach several hundred eV during the application of HHFW. The peak emissivity locations for the heated edge ions are located just inside the LCFS. Hence, their orbits can carry them into the plasma SOL and possibly provide a significant loss of ions and RF power.

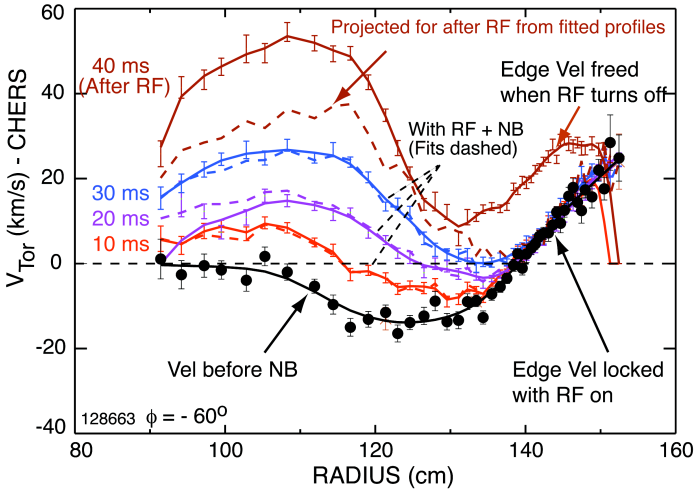

FIGURE 2. Toroidal velocity of C VI versus radius for the -60° deuterium case of Fig. 1. The intrinsic V_{tor} with RF only is a function of radius. Edge V_{tor} is clamped with RF on.

An indication that energetic ions are being lost from the plasma edge is given by the charge exchange recombination spectroscopy (CHERS) [15] measurements of toroidal velocity (V_{tor}). Profiles of V_{tor} for C VI ions, obtained with a 40 ms, 2 MW "diagnostic" neutral beam pulse (NBI) overlapping the end of a 1.1 MW RF pulse by 30 ms, are given in Fig. 2 (-60° case of Fig.1). These measurements reveal that the

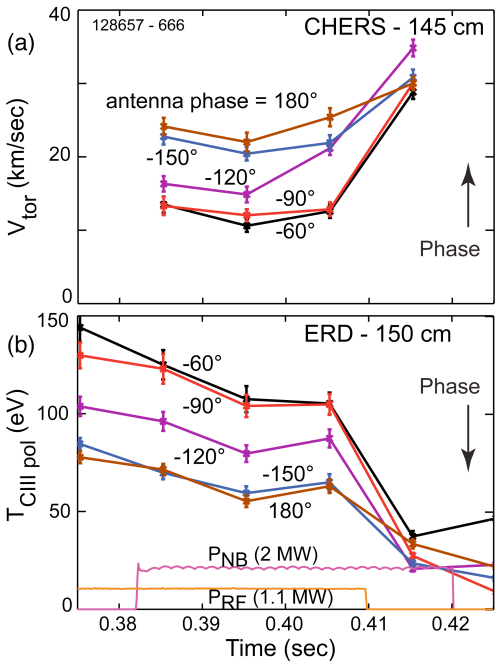

FIGURE 3. Phase scans of a) CHERS V_{tor} at R = 145 cm and ERD poloidal $T_{C\ III}$ in the plasma edge (R=150 cm) for the deuterium plasma antenna phase scan of Fig. 1.

edge velocity is "clamped" during the three 10 ms time slots with the RF applied and is subsequently released during the last 10 ms time slot with no RF applied. This points to a possible effect of the loss of the energetic ions heated perpendicular to the magnetic field by the PDI [13].

Further evidence that this edge clamping is associated with energetic edge ion loss is provided by the phase scan of edge V_{tor} compared to the level of energetic ion heating at the LCFS as shown in Fig. 3. Edge V_{tor} at a major radius of R = 145 cm is generally clamped in Fig. 4a with HHFW applied during the beam pulse for a ϕ_A range of – 60° to – 150° (ϕ_A scan of Fig.1). The clamped level of this velocity increases with antenna phase, and with the removal of the RF this velocity quickly accelerates to approximately the same level with NBI alone. Concurrently, the edge poloidal C III temperature (single Gaussian fit) at the peak of the emissivity at R = 150 cm increases as the antenna phase is decreased and returns to the level without applied RF power very quickly at the turn off of the RF pulse. The correspondence between higher edge ion energy and the reduction of the edge V_{tor} clamp level suggests that energetic ion loss to the SOL is significant.

III. HHFW POWER COUPLING TO H-MODE PLASMAS

Power Coupled to Core Plasma Versus Antenna Phase

With the introduction of lithium into NSTX, the density level in the SOL is reduced considerably permitting significant HHFW electron heating in the deuterium H-mode plasma for the first time. Earlier H-mode results taken without extensive conditioning indicated some ion heating but no observable electron heating [16]. Core electron heating peaked on axis has been obtained with minimal fresh lithium conditioning [12]. However, when the lithium conditioning is sustained during the HHFW heating run, the electron heating shifts off axis as is indicated in Fig. 4 for two antenna phase conditions ϕ_A = -150° and -90° (k_ϕ = -13 m^{-1} and 8 m^{-1}, respectively). Incremental electron heating (pressure) increases from the axis of the plasma toward the top of the pedestal for both antenna phases. The increments in electron and total stored energies at the higher phase are about twice the levels obtained for the lower phase case: ΔW_e ~ 13 kJ, 7 kJ and ΔW_{tot} ~ 25 kJ, 14 kJ for ϕ_A = -150°, -90°. As expected, if the propagating fast waves are contributing to edge losses [8], the average edge density <edge n_e> near the antenna (measured with Thomson scattering at R=156.2 cm) is less

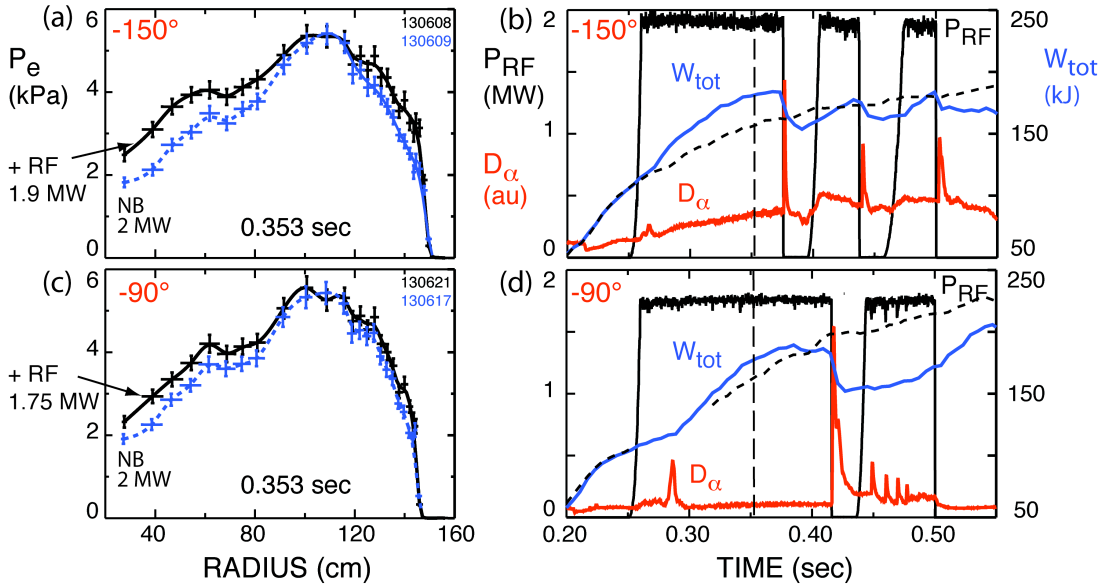

FIGURE 4. Left panels: electron pressure profiles at t = 0.353 sec with and without RF power for ϕ_A = -150° and -90°. Right panels: coupling properties for these H-mode shots showing stored energy with and without RF power and reduction of stored energy due to type I ELMs. (P_{NB} = 2 MW, I_P = 1 MA, B_ϕ = 0.55 T)

than the n_{onset} value for the -150° case, ~ 0.70x10^{18} m^{-3}, and above the n_{onset} value for the -90° case, ~ 0.71x10^{18} m^{-3}. An exponential fit to the ΔW_{tot} data versus time [8] indicates an energy confinement time of ~ 20 ms for both the ϕ_A = -150° and -90° cases. Thus, the calculated values for the core power deposition P_{RFdep} in the two cases are ~ 1.2 MW at ϕ_A = -150° and ~ 0.7 MW at ϕ_A = -90°, giving values of power lost to the edge region P_{RFedge} of ~ 0.7 MW, ~ 1.1 MW for the ϕ_A = -150° and -90° cases, respectively. Some of this loss is through the PDI channel as discussed earlier. However, a substantial edge power loss must be occurring through fast wave losses, which are a strong function of k_ϕ, as indicated here.

With a fast visible color camera view of the NSTX plasma cross-section, an important edge RF power loss channel from the SOL region in front of the HHFW antenna to the lower outer divertor plate has been discovered, as shown in Fig. 5. Streaming of RF power along the magnetic field lines to the lower divertor plate occurs at both phases. The "hot" interaction region on the lower divertor plate is more pronounced for ϕ_A = -90° than for -150°, consistent with the greater edge power loss at -90° and the greater separation between n_{onset} and the wall at ϕ_A = -150°. Furthermore, the time for the "hot"

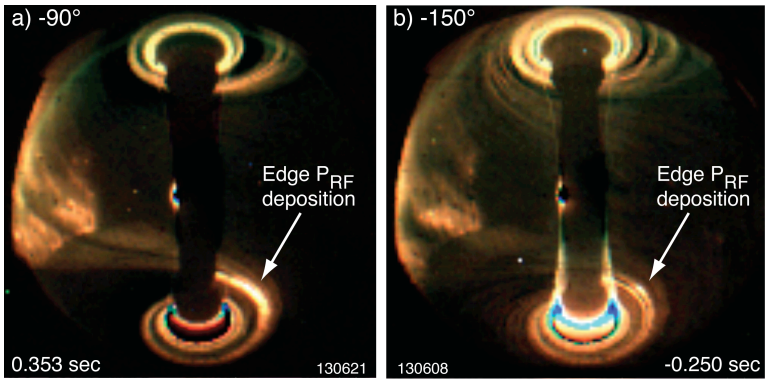

FIGURE 5. Visible camera frames taken for the left panels of Fig. 4 (t = 0.353 sec) with the NB background frame at 0.250 sec subtracted.

region to decay away after the removal of the RF power is considerably longer for the ϕ_A = -90° case: ~ 20 ms compared to ~ 8 ms for the ϕ_A = -150° case. Infrared emission measurements across the "hot" zones give heat fluxes consistent with hundreds of kilowatts of RF power being lost to the divertor plate.

ELM Characteristics

As indicated in Fig. 4, all three RF pulses at ϕ_A = -150° and the first RF pulse at ϕ_A = -90° lead to large type I ELMs, accompanied by large drops in stored energy (~ - 20% for the first RF pulses) as is typical for the type I ELM [17]. It is necessary to understand the ELM behavior with HHFW heating, and how to avoid them or be resilient to them [18], in order to optimize HHFW power coupling to the core H-mode plasma. Expansion of the time scale of the ELM regions following the first RF pulses for the two antenna phases shows that the lower divertor view D_α spectroscopic signals for the ELMs increase only after the RF power is switched off due to high voltage arcs inside the antenna. It is not clear what causes the arcs, but it is suspected that blobs [19, 20] or dust particles [21] enter the antenna through the 50% open Faraday shield. As will become evident below, the ELMs do not cause the RF to be removed by increasing the density in front of the antenna in these cases.

Relatively fast characteristics for the ELM at the end of the first RF pulse for the ϕ_A = -150° case of Fig. 4b are shown in Fig 6: the edge cord ultra-soft X-ray (USXR) signal taken without a Be filter (bolometer mode) near the LCFS (XHD14) which is approximately $\propto n_e^2$ [20]; a mid-plane D_α signal (D_α mid) from a view directed toward the NSTX center-stack; and the even n integrated mid-frequency (60-300 kHz) MHD signal (emidf). The D_α mid signal for the ELM closely follows the peaking of the XHD14 signal, and both peak up much faster than that of the divertor D_α signal (D_α div). D_α mid responds to the ELM density as opposed to the loss of core energy which drives the rise of D_α div over the longer period of ~ 1.5 ms. The emidf signal shows the MHD oscillation characteristic of the ELM [22, 23] that accompanies the large rise of the ELM on the XHD14 signal. Precursors are evident on all three signals during the 0.2 ms time frame of the arc (P_{RF} is sampled here at 5 kHz). The XHD14 signal gives the clearest indication and there is a hint of an increase for D_α mid. Finally, there is considerable emidf MHD activity during the arc time frame, suggesting that a pre-ELM event could be responsible for the injection of plasma or dust into the antenna, thereby causing the arc. Note however that some emidf MHD bursts occur before the arc without causing an arc.

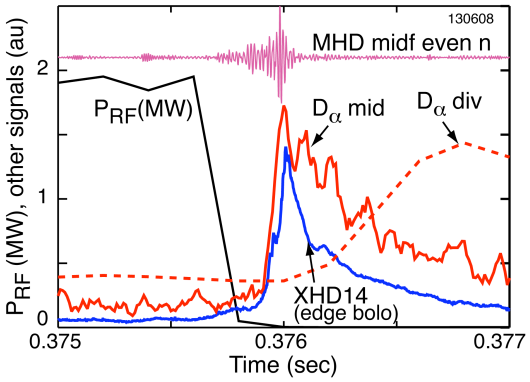

FIGURE 6. Characteristics for the ELM at the end of the first RF pulse in Fig. 4b as described in the text. (ϕ_A = -150°)

Even though precursors may be causing the arc in Fig. 6, it is observed that type I ELMs can occur after the removal of the RF power, either by an arc or by cutting off

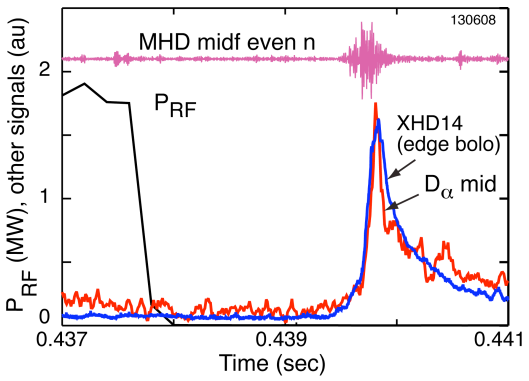

FIGURE 7. Characteristics for the ELM at the end of the second RF pulse in Fig. 4b as described in the text. (ϕ_A = -150°)

the RF pulse, without apparent precursors as found for the last two RF pulses of the ϕ_A = -150° case in Fig. 4b. Figure 7 shows that the ELM following the second RF pulse occurs about 1.5 ms after the arc. Note that the emidf MHD activity is quite low during the interim period. Furthermore, the usual helical ELM structure is not observed with the fast camera prior to the ELM buildup. This delay of the ELM response suggests a relaxation of the pressure, current profile, or energetic ion characteristics of the discharge may be leading to the ELM. This behavior contrasts with that observed on ASDEX Upgrade [24] for which the timing of the ELMs was less directly correlated with that of the arcs. Arcs do not always lead to ELMs on NSTX, but it is clear that arcs must be prevented if large ELMs are to be avoided.

Coupling Power in the Presence of Large ELMs

By lowering the RF power/antenna voltage somewhat and increasing the RF source reflection coefficient trip points to 0.7, it is possible to maintain RF power through a large type I ELM, as shown in Fig. 8 for ϕ_A = -90° with P_{RF} = 1.3 MW. The ELM affects the HHFW power coupled by increasing the density in front of the antenna, which in turn increases the source reflection coefficients. The ELM in this case has a double peak structure (two ELMs) as indicated by the XHD14 and XHD13 (the next chord farther inboard from the plasma edge) signals that are indicative of the density in the edge region. Note that these peaks correspond to peaks observed on the representative source #3 reflection coefficient and to the two larger drops in the RF power coupled.

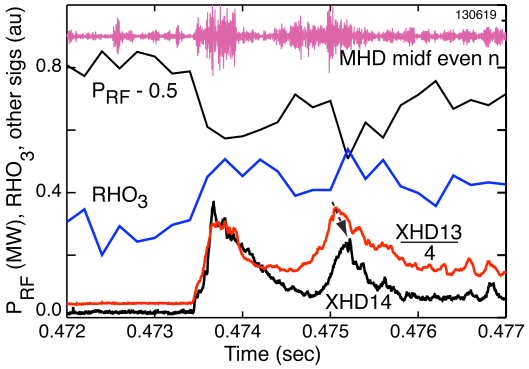

FIGURE 8. Effect of large type I ELM (s) on P_{RF} and the source #3 reflection coefficient. (P_{NB} = 2 MW, I_P = 1 MA, B_ϕ = 0.55 T)

Even though the digitization of the RF signals is rather slow in Fig. 8 (5 kHz), it is still clear that the rise time of the reflection coefficients is of the order of ~ 100 μs and thus much longer than that for a high-voltage arc, ≤ ~ 10 μs. Therefore, it is possible in principle to apply RF heating through ELMs with the HHFW system on NSTX using arc/ELM discrimination based on the detection of the derivatives of the source reflection coefficients. This could prove to be a viable alternative to ELM resilient systems now being used [18] or being planned for ITER [25] and will be implemented on NSTX.

IV. POSSIBLE IMPLICATIONS FOR ITER

The most important implication of the NSTX edge loss results for ITER is that the edge losses from fast wave edge fields could prove to be significant. For ITER the onset density for perpendicular fast wave propagation for $\phi_A = 90°$ is only ~ 1.4 x 10^{18} m^{-3}. It could prove to be difficult to keep the edge density this low and, as a consequence, a non-negligible power could be deposited in the divertor region, as shown in Fig. 5, resulting in serious sputtering and erosion during long pulse operation. If gas puffing is used to enhance loading to keep the antenna voltages at acceptable levels [26], the edge density level will need to be chosen to balance antenna loading versus the enhancement of edge power losses. Benchmarking of advanced RF codes that include all the edge fast wave fields against quantitative first-pass edge power deposition data to be obtained on NSTX is needed to predict the severity of edge power losses for the different operating scenarios on ITER.

ACKNOWLEDGEMENTS

The authors wish to acknowledge the support of Dr. Masayuki Ono and Dr. Jonathan Menard, the NSTX team and the machine, RF, and neutral beam operations groups. This work is supported by USDOE Contract No. DE-AC02-09CH11466.

REFERENCES

1. J.E. Stevens *et al., Plasma Phys. and Control. Fusion* **32** (1990) 189.
2. M Bures *et al., Plasma Phys. and Control. Fusion* **33** (1991) 937.
3. L. Colas *et al*., *AIP Conference Proceedings* **787** (2005) 150.
4. J-M. Noterdaeme *et al*., *Fusion Engineering Design* **12** (1990) 127.
5. S. J. Wukitch *et al., AIP Conference Proceedings* **933** (2007) 75.
6. A.P. Smirnov and R.W. Harvey, *Bull. Am. Phys. Soc.* **40** (1995) 1837.
7. E. F. Jaeger *et al., Physics of Plasmas* **8** (2001) 1573.
8. J.C. Hosea, *et al.*, *Physics of Plasmas* **15** (2008) 056104.
9. C.K. Phillips, *et al.*, *Nuclear Fusion* **49** (2009) 075015.
10. H.W. Kugel *et al., Journal of Nuclear Materials* **390–391** (2009) 1000.
11. E. Mazzucato *et al., Nucear Fusion* **49** (2009) 055001.
12. G. Taylor, *et al.*, this conference.
13. T.M. Biewer *et al.*, *Physics of Plasmas* **12**, (2005) 056108.
14. J.R. Wilson *et al.*, *AIP Conference Proceedings* **787** (2005) 66.
15. R.E. Bell, *Review of Scientific Instruments* **77** (2006) 10E902.
16. B.P. LeBlanc *et al.*, *AIP Conference Proceedings* **787** (2005) 86.
17. K. Tritz *et al., Physics of Plasmas* **15** (2008) 056119.
18. M. Vrancken *et al*., *Fusion Engineering and Design* **82** (2007) 873.
19. S.J. Zweben et *al*., *IEEE Trans. on Plasma Science* **33** (2005) 446.
20. R. Maingi *et al.*, *Physics of Plasmas* **13** (2006) 092510.
21. A.L. Roquemore *et al., Journal of Nuclear Materials* **363–365** (2007) 222.
22. R. Maingi *et al*., Nuclear Fusion **45** (2005) 1066.
23. J. Neuhauser *et al., Nucl. Fusion* **48** (2008) 045005.
24. Vl.V. Bobkov *et al., Journal of Nuclear Materials* **337-339** (2005) 776.
25. D.W. Swain and R. Goulding, *Fusion Engineering and Design* **82** (2007) 603.
26. M-L. Mayoral *et al., AIP Conference Proceedings* 933 (2007) 55.

The Princeton Plasma Physics Laboratory is operated
by Princeton University under contract
with the U.S. Department of Energy.

Information Services
Princeton Plasma Physics Laboratory
P.O. Box 451
Princeton, NJ 08543

Phone: 609-243-2750
Fax: 609-243-2751
e-mail: pppl_info@pppl.gov
Internet Address: http://www.pppl.gov